Available online at www.sciencedirect.com

ScienceDirect

International Journal of Heat and Mass Transfer 51 (2008) 1658–1664

International Journal of HEAT and MASS TRANSFER

www.elsevier.com/locate/ijhmt

Natural convection about a vertical plate embedded in a bidisperse porous medium

D.A. Nield [a], A.V. Kuznetsov [b,*]

[a] Department of Engineering Science, University of Auckland, Private Bag 92019, Auckland 1142, New Zealand
[b] Department of Mechanical and Aerospace Engineering, North Carolina State University, Campus Box 7910, Raleigh, NC 27695-7910, USA

Received 21 May 2007; received in revised form 12 July 2007
Available online 11 September 2007

Abstract

The classical Cheng–Minkowycz study of convection past a vertical plate embedded in a porous medium has been extended to the case of a bidisperse porous medium (BDPM). The boundary layer analysis leads to expressions for the velocity and temperature fields in terms of a geometrical parameter, an inter-phase momentum transfer parameter, a thermal diffusivity ratio, a permeability ratio, a thermal conductivity ratio, and an inter-phase heat transfer parameter. For the leading edge region, and for an inner layer, a similarity solution is obtained numerically. This involves the first four parameters, each of which is a characteristic of the BDPM.

1. Introduction

A bidisperse porous medium (BDPM, see Fig. 1), as informally defined by Chen et al. [1,2], is composed of clusters of large particles that are agglomerations of small particles. Thus there are macro-pores between the clusters and micro-pores within them. Applications are found in bidisperse adsorbent or bidisperse capillary wicks in a heat pipe. Since the bidisperse wick structure significantly increases the area available for liquid film evaporation, it has been proposed for use in the evaporator of heat pipes.

A BDPM may thus be looked at as a standard porous medium in which the solid phase is replaced by another porous medium, whose temperature may be denoted by T_p if local thermal equilibrium is assumed within each cluster. We can then talk about the f-phase (the macro-pores) and the p-phase (the remainder of the structure). An alternative way of looking at the structure is to regard it as a porous medium in which fractures or tunnels have been introduced. One can then think of the f-phase as being a 'fracture phase' and the p-phase as being a 'porous phase'.

The Darcy model for the steady-state momentum transfer in a BDPM is represented by the following pair of coupled equations for the Darcy velocities $\mathbf{v}_f^*$ and $\mathbf{v}_p^*$, where the asterisks denote dimensional variables

$$\mathbf{G} = \left(\frac{\mu}{K_f}\right)\mathbf{v}_f^* + \zeta(\mathbf{v}_f^* - \mathbf{v}_p^*), \tag{1a}$$

$$\mathbf{G} = \left(\frac{\mu}{K_p}\right)\mathbf{v}_p^* + \zeta(\mathbf{v}_p^* - \mathbf{v}_f^*). \tag{1b}$$

Here $\mathbf{G}$ is the negative of the applied pressure gradient, μ is the fluid viscosity, K_f and K_p are the permeabilities of the two phases, and ζ is the coefficient for momentum transfer between the two phases.

These equations were applied by Nield and Kuznetsov [3,4] to forced convection in a channel and by Nield and Kuznetsov [5] to the Horton–Rogers–Lapwood problem (the paradigmatic problem for natural convection in an enclosed region). These studies were reviewed by Nield and Kuznetsov [6].

In this paper we apply the two-velocity two-temperature formulation to a problem that is paradigmatic for external natural convection in a porous medium, namely the problem of convection past a vertical plate, a problem first considered by Cheng and Minkowycz [7]. The problem leads

* Corresponding author.
E-mail address: avkuznet@eos.ncsu.edu (A.V. Kuznetsov).

0017-9310/$ - see front matter
doi:10.1016/j.ijheatmasstransfer.2007.07.011

Nomenclature

c	specific heat at constant pressure
d	characteristic length scale
$\mathbf{G}$	negative of the applied pressure gradient
g	gravitational acceleration
h	inter-phase heat transfer coefficient (incorporating the specific area)
$\hat{h}$	dimensionless inter-phase heat transfer parameter, $hd^2/\phi k_f$
H	$\hat{h}/R$
k	thermal conductivity
K	permeability
K_r	permeability ratio, K_p/K_f
R	Rayleigh number, $\frac{\rho_F g\hat{\beta}(T_w-T_\infty)K_f d}{\mu\phi k_f/(\rho c)_f}$
T_∞	ambient temperature
T_w	wall temperature
$\mathbf{v}^*$	filtration velocity

Greek symbols

α	thermal diffusivity ratio, $\frac{k_f}{k_p}\frac{(\rho c)_p}{(\rho c)_f}$
β	modified thermal capacity ratio, $\frac{(1-\phi)k_p(\rho c)_f}{\phi k_f(\rho c)_p}$
$\hat{\beta}$	volumetric thermal expansion coefficient of the fluid
γ	modified thermal conductivity ratio, $\frac{\phi k_f}{(1-\phi)k_p}$
ε	porosity within the p-phase
ζ	coefficient for momentum transfer between the two phases
η	boundary-layer parameter
μ	fluid viscosity
ρ_F	density of the fluid
σ_f	f-phase momentum transfer parameter, $\frac{\zeta K_f}{\mu}$
τ	$\frac{\phi}{\phi+(1-\phi)\varepsilon}$
ϕ	volume fraction of the f-phase

Subscripts

f	fracture phase (macro-pores)
p	porous phase (micro-pores)

Superscripts

*	dimensional variable

naturally to a boundary-layer formulation. We are guided by a study using a model involving two temperatures (local thermal non-equilibrium) but a single velocity by Rees and Pop [8]. Related work is presented in [9–12]. For the more general aspects of convection in a porous medium past a vertical plate the reader is referred to the survey in Section 5.1 of Nield and Bejan [13]. It is also worth mentioning that similar work involving local thermal non-equilibrium for the geometry of the Horton–Rogers–Lapwood problem has been surveyed in Section 6.5 of [13].

2. Analysis

We consider steady two-dimensional flow in a BDPM induced by a vertical heated plate held at the constant temperature T_w and embedded in the BDPM with ambient temperature T_∞. In the following analysis asterisks denote dimensional variables. The plate is taken to lie along the positive x^*-axis. The configuration is standard, and the reader is referred to Figure 5.1 of [13] or Figure 1 of [7]. The equations of continuity (expressing conservation of mass) for the velocity components in the two phases are

$$\frac{\partial u_f^*}{\partial x^*}+\frac{\partial v_f^*}{\partial y^*}=0, \tag{2a}$$

$$\frac{\partial u_p^*}{\partial x^*}+\frac{\partial v_p^*}{\partial y^*}=0. \tag{2b}$$

We note that in the traditional Darcy formulation the pressure is an intrinsic quantity, i.e. it is the pressure in the fluid. We recognize that in a BDPM the fluid occupies all of the f-phase and a fraction of the p-phase. We denote the volume fraction of the f-phase by ϕ (something that in a regular porous medium would be called the porosity) and the porosity in the p-phase by ε. Thus $1-\phi$ is the volume fraction of the p-phase, and the volume fraction of the BDPM occupied by the fluid is $\phi+(1-\phi)\varepsilon$. The volume average of the temperature over the fluid is

$$T_F^*=\frac{\phi T_f^*+(1-\phi)\varepsilon T_p^*}{\phi+(1-\phi)\varepsilon}. \tag{3}$$

The drag force (per unit volume) balances the gradient of the excess pressure over hydrostatic. Our basic hypothesis is that in a BDPM the drag is increased by an amount $\zeta(\mathbf{v}_f^*-\mathbf{v}_p^*)$ for the f-phase and decreased by the same amount for the p-phase. Accordingly, we write the momentum equations as

$$\frac{\partial p^*}{\partial x^*}=-\frac{\mu}{K_f}u_f^*-\zeta(u_f^*-u_p^*)+\rho_F g\hat{\beta}(T_F^*-T_\infty), \tag{4a}$$

$$\frac{\partial p^*}{\partial x^*}=-\frac{\mu}{K_p}u_p^*-\zeta(u_p^*-u_f^*)+\rho_F g\hat{\beta}(T_F^*-T_\infty), \tag{4b}$$

$$\frac{\partial p^*}{\partial y^*}=-\frac{\mu}{K_f}v_f^*-\zeta(v_f^*-v_p^*), \tag{4c}$$

$$\frac{\partial p^*}{\partial y^*}=-\frac{\mu}{K_p}v_p^*-\zeta(v_p^*-v_f^*). \tag{4d}$$

Here ρ_F is the density of the fluid and $\hat{\beta}$ is the volumetric thermal expansion coefficient of the fluid.

The thermal energy equations are taken as

$$\phi(\rho c)_f\mathbf{v}_f^*\cdot\nabla T_f^*=\phi k_f\nabla^2T_f^*+h(T_p^*-T_f^*), \tag{5a}$$

$$(1-\phi)(\rho c)_p\mathbf{v}_p^*\cdot\nabla T_p^*=(1-\phi)k_p\nabla^2T_p^*+h(T_f^*-T_p^*). \tag{5b}$$

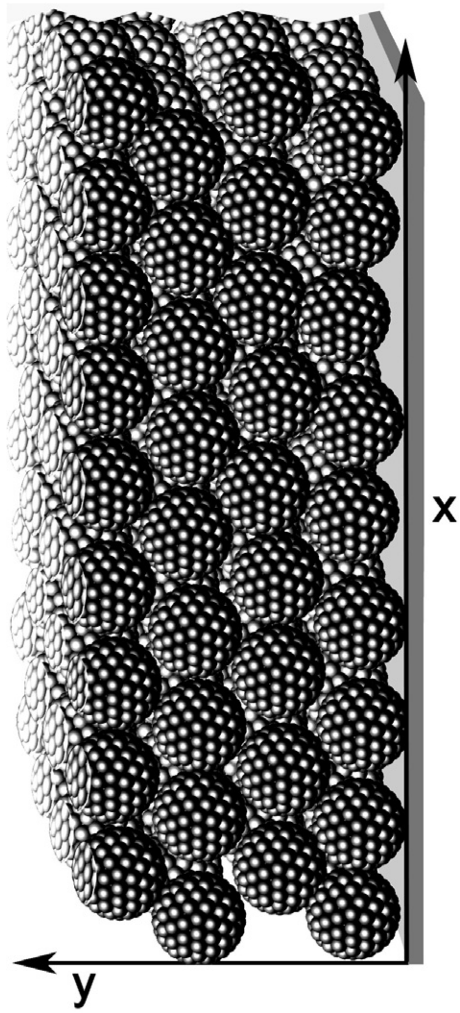

Fig. 1. Sketch of a bidisperse porous medium adjacent to a vertical plate.

Here c denotes the specific heat at constant pressure, k denotes the thermal conductivity, and h is an inter-phase heat transfer coefficient (incorporating the specific area).

We introduce dimensionless variables as follows:

$$(x^*, y^*) = d(\hat{x}, \hat{y}), \quad p^* = \frac{k_f \mu}{(\rho c)_f K_f} p, \tag{6}$$

$$(u_f^*, v_f^*) = \frac{\phi k_f}{(\rho c)_f d}(\hat{u}_f, \hat{v}_f), \quad (u_p^*, v_p^*) = \frac{(1-\phi) k_p}{(\rho c)_p d}(\hat{u}_p, \hat{v}_p), \tag{7}$$

$$T_f^* = (T_w - T_\infty)\theta_f + T_\infty, \quad T_p^* = (T_w - T_\infty)\theta_p + T_\infty. \tag{8}$$

We introduce the stream functions $\hat{\psi}_f$ and $\hat{\psi}_p$ defined so that

$$\hat{u}_f = -\frac{\partial \hat{\psi}_f}{\partial \hat{y}}, \quad \hat{v}_f = \frac{\partial \hat{\psi}_f}{\partial \hat{x}}, \quad \hat{u}_p = -\frac{\partial \hat{\psi}_p}{\partial \hat{y}}, \quad \hat{v}_p = \frac{\partial \hat{\psi}_p}{\partial \hat{x}}. \tag{9}$$

(We use the sign convention in [8] rather than that in [5].)

We define a Rayleigh number R based on properties in the f-phase by

$$R = \frac{\rho_F g \hat{\beta} (T_w - T_\infty) K_f d}{\mu \phi k_f / (\rho c)_f}. \tag{10}$$

Elimination of the pressure from Eqs. (4a–d) then leads to

$$(1+\sigma_f)\nabla^2 \hat{\psi}_f - \beta \sigma_f \nabla^2 \hat{\psi}_p = R \frac{\partial \theta_F}{\partial \hat{y}}, \tag{11a}$$

$$-\sigma_f \nabla^2 \hat{\psi}_f + \beta \left(\frac{1}{K_r} + \sigma_f \right) \nabla^2 \hat{\psi}_p = R \frac{\partial \theta_F}{\partial \hat{y}}, \tag{11b}$$

where

$$\frac{\partial \theta_F}{\partial \hat{x}} = \frac{\phi \frac{\partial \theta_f}{\partial \hat{x}} + (1-\phi)\varepsilon \frac{\partial \theta_p}{\partial \hat{x}}}{\phi + (1-\phi)\varepsilon}. \tag{12}$$

Here we have introduced the dimensionless parameters

$$\sigma_f = \frac{\zeta K_f}{\mu}, \quad \beta = \frac{(1-\phi) k_p (\rho c)_f}{\phi k_f (\rho c)_p}. \tag{13}$$

Thus σ_f is an inter-phase momentum transfer parameter, while β is a modified thermal diffusivity ratio.

Also, the thermal energy equations (5a,b) become

$$\nabla^2 \theta_f = \hat{h}(\theta_f - \theta_p) + \frac{\partial \hat{\psi}_f}{\partial \hat{y}} \frac{\partial \theta_f}{\partial \hat{x}} - \frac{\partial \hat{\psi}_f}{\partial \hat{x}} \frac{\partial \theta_f}{\partial \hat{y}}, \tag{14a}$$

$$\nabla^2 \theta_p = \gamma \hat{h}(\theta_p - \theta_f) + \frac{\partial \hat{\psi}_p}{\partial \hat{y}} \frac{\partial \theta_p}{\partial \hat{x}} - \frac{\partial \hat{\psi}_p}{\partial \hat{x}} \frac{\partial \theta_p}{\partial \hat{y}}, \tag{14b}$$

where

$$\gamma = \frac{\phi k_f}{(1-\phi) k_p}, \quad \hat{h} = \frac{h d^2}{\phi k_f}. \tag{15}$$

Thus γ is a modified thermal conductivity ratio and $\hat{h}$ is an inter-phase heat transfer parameter.

Next we introduce the boundary-layer scaling

$$\hat{x} = x, \quad \hat{y} = R^{-1/2} y, \quad \hat{\psi}_f = R^{1/2} \psi_f, \quad \hat{\psi}_p = R^{1/2} \psi_p, \tag{16}$$

and the shorthand

$$\tau = \frac{\phi}{\phi + (1-\phi)\varepsilon}, \quad K_r = \frac{K_p}{K_f}. \tag{17}$$

Then we get

$$(1+\sigma_f) \frac{\partial^2 \hat{\psi}_f}{\partial y^2} - \beta \sigma_f \frac{\partial^2 \hat{\psi}_p}{\partial y^2} = \tau \frac{\partial \theta_f}{\partial y} + (1-\tau) \frac{\partial \theta_p}{\partial y}, \tag{18a}$$

$$-\sigma_f \frac{\partial^2 \hat{\psi}_f}{\partial y^2} + \beta \left(\frac{1}{K_r} + \sigma_f \right) \frac{\partial^2 \hat{\psi}_p}{\partial y^2} = \tau \frac{\partial \theta_f}{\partial y} + (1-\tau) \frac{\partial \theta_p}{\partial y}, \tag{18b}$$

$$\frac{\partial^2 \theta_f}{\partial y^2} = H(\theta_f - \theta_p) + \frac{\partial \psi_f}{\partial y} \frac{\partial \theta_f}{\partial x} - \frac{\partial \psi_f}{\partial x} \frac{\partial \theta_f}{\partial y}, \tag{18c}$$

$$\frac{\partial^2 \theta_p}{\partial y^2} = \gamma H(\theta_p - \theta_f) + \frac{\partial \psi_p}{\partial y} \frac{\partial \theta_p}{\partial x} - \frac{\partial \psi_p}{\partial x} \frac{\partial \theta_p}{\partial y}, \tag{18d}$$

where

$$H = \hat{h}/R. \tag{19}$$

In moving from Eqs. (14a,b) to (18c,d) we have made the usual boundary-layer approximation that conduction in the x-direction is negligible in comparison to that in the y-direction.

The appropriate boundary conditions are

$$\psi_{\mathrm{f}} = 0, \quad \psi_{\mathrm{p}} = 0, \quad \theta_{\mathrm{f}} = 1, \quad \theta_{\mathrm{p}} = 1 \quad \text{at } y = 0, \tag{20a}$$

$$\frac{\partial \psi_{\mathrm{f}}}{\partial y}, \quad \frac{\partial \psi_{\mathrm{p}}}{\partial y}, \quad \theta_{\mathrm{f}}, \quad \theta_{\mathrm{p}} \to 0 \quad \text{as } y \to \infty. \tag{20b}$$

These boundary conditions allow Eqs. (18a,b) to be integrated once to yield

$$(1+\sigma_{\mathrm{f}})\frac{\partial \hat{\psi}_{\mathrm{f}}}{\partial y} - \beta\sigma_{\mathrm{f}}\frac{\partial \hat{\psi}_{\mathrm{p}}}{\partial y} = \tau\theta_{\mathrm{f}} + (1-\tau)\theta_{\mathrm{p}}, \tag{21a}$$

$$-\sigma_{\mathrm{f}}\frac{\partial \hat{\psi}_{\mathrm{f}}}{\partial y} + \beta\left(\frac{1}{K_{\mathrm{r}}} + \sigma_{\mathrm{f}}\right)\frac{\partial \hat{\psi}_{\mathrm{p}}}{\partial y} = \tau\theta_{\mathrm{f}} + (1-\tau)\theta_{\mathrm{p}}. \tag{21b}$$

We now introduce the usual boundary-layer transformation appropriate to the Cheng–Minkowycz problem

$$\psi_{\mathrm{f}} = x^{1/2} f(x,\eta), \quad \psi_{\mathrm{p}} = x^{1/2} g(x,\eta), \tag{22a}$$

$$\theta_{\mathrm{f}} = \theta_{\mathrm{f}}(x,\eta), \quad \theta_{\mathrm{p}} = \theta_{\mathrm{p}}(x,\eta), \tag{22b}$$

where

$$\eta = \frac{y}{x^{1/2}}. \tag{23}$$

One then has the system

$$(1+\sigma_{\mathrm{f}})f' - \beta\sigma_{\mathrm{f}} g' = \tau\theta_{\mathrm{f}} + (1-\tau)\theta_{\mathrm{p}}, \tag{24a}$$

$$-\sigma_{\mathrm{f}} f' + \beta\left(\frac{1}{K_{\mathrm{r}}} + \sigma_{\mathrm{f}}\right) g' = \tau\theta_{\mathrm{f}} + (1-\tau)\theta_{\mathrm{p}}, \tag{24b}$$

$$\theta_{\mathrm{f}}'' + \frac{1}{2} f\theta_{\mathrm{f}}' = Hx(\theta_{\mathrm{f}} - \theta_{\mathrm{p}}) + x(f'\theta_{\mathrm{f}x} - \theta_{\mathrm{f}} f_x), \tag{24c}$$

$$\theta_{\mathrm{p}}'' + \frac{1}{2} g\theta_{\mathrm{p}}' = \gamma Hx(\theta_{\mathrm{p}} - \theta_{\mathrm{f}}) + x(g'\theta_{\mathrm{p}x} - \theta_{\mathrm{p}} g_x), \tag{24d}$$

subject to the boundary conditions

$$f = 0, \quad g = 0, \quad \theta_{\mathrm{f}} = 1, \quad \theta_{\mathrm{p}} = 1 \quad \text{at } \eta = 0, \tag{24e}$$

$$\theta_{\mathrm{f}}, \quad \theta_{\mathrm{p}} \to 0 \quad \text{as } \eta \to \infty. \tag{24f}$$

It is worth noting that the boundary conditions (24f) together with (24a) and (24b) imply that $f', g' \to 0$ as $\eta \to \infty$.

In these equations the primes denote derivatives with respect to η and the x-subscripts denote derivatives with respect to x.

3. Asymptotic analysis near the leading edge

We continue to follow Rees and Pop [8]. The small-x analysis is facilitated by setting

$$\psi_{\mathrm{f}} = x^{1/2} F(x,y), \quad \psi_{\mathrm{p}} = x^{1/2} G(x,y), \tag{25a}$$

$$\theta_{\mathrm{f}} = \Theta_{\mathrm{f}}(x,y), \quad \theta_{\mathrm{p}} = \Theta_{\mathrm{p}}(x,y), \tag{25b}$$

in Eqs. (21a,b) and (18c,d), which become

Table 1
Numerical results obtained from the solution of the system (31) for $\phi = 0.4$, $\varepsilon = 0.4$, and so for $\tau = 0.625$

Case	σ_{f}	β	K_{r}	$f_0(\infty)$	$g_0(\infty)$	$-\theta_{\mathrm{f0}}'(0)$	$-\theta_{\mathrm{p0}}'(0)$	$-\phi\theta_{\mathrm{f0}}'(0) - (1-\phi)\theta_{\mathrm{p0}}'(0)$
1	0.0001	0.1	0.0001	2.75136	0.00275	0.48226	0.10041	0.25315
2	0.0001	0.1	0.01	2.47119	0.24717	0.47731	0.14151	0.27583
3	0.0001	0.1	1	1.32878	13.28780	0.39041	1.58962	1.10993
4	0.0001	1	0.0001	2.75423	0.000275	0.48231	0.10004	0.25295
5	0.0001	1	0.01	2.72297	0.027235	0.48182	0.10409	0.25518
6	0.0001	1	1	1.61154	1.61154	0.44390	0.44390	0.44390
7	0.0001	10	0.0001	2.75452	0.000027	0.48231	0.10000	0.25293
8	0.0001	10	0.01	2.75136	0.00275	0.48226	0.100408	0.25315
9	0.0001	10	1	2.47142	0.24714	0.47734	0.14151	0.27584
10	0.01	0.1	0.0001	2.72886	0.00278	0.47983	0.10041	0.25218
11	0.01	0.1	0.01	2.44897	0.24974	0.47484	0.14199	0.27513
12	0.01	0.1	1	1.32878	13.28780	0.39041	1.58961	1.10993
13	0.01	1	0.0001	2.73173	0.00028	0.47987	0.10004	0.25197
14	0.01	1	0.01	2.70066	0.02754	0.47940	0.10414	0.25425
15	0.01	1	1	1.61153	1.61153	0.44390	0.44390	0.44390
16	0.01	10	0.0001	2.73202	0.000028	0.47987	0.10000	0.25195
17	0.01	10	0.01	2.72909	0.00278	0.47985	0.10041	0.25219
18	0.01	10	1	2.47142	0.247142	0.47734	0.14151	0.27584
19	1	0.1	0.0001	1.56692	0.00470	0.33740	0.10069	0.19538
20	1	0.1	0.01	1.37194	0.40351	0.33213	0.16982	0.23475
21	1	0.1	1	1.32878	13.28780	0.39040	1.58962	1.10993
22	1	1	0.0001	1.56927	0.00047	0.33748	0.10007	0.19503
23	1	1	0.01	1.56196	0.04594	0.33925	0.10689	0.19983
24	1	1	1	1.61154	1.61154	0.44390	0.44390	0.44390
25	1	10	0.0001	1.56951	0.00005	0.33748	0.10001	0.19500
26	1	10	0.01	1.58527	0.00466	0.33997	0.10069	0.19640
27	1	10	1	2.47142	0.247142	0.47734	0.14151	0.27584

$$(1+\sigma_f)x^{1/2}F_y - \beta\sigma_f x^{1/2}G_y = \tau\Theta_f + (1-\tau)\Theta_p, \tag{26a}$$

$$-\sigma_f x^{1/2}F_y + \beta\left(\frac{1}{K_r}+\sigma_f\right)x^{1/2}G_y = \tau\Theta_f + (1-\tau)\Theta_p, \tag{26b}$$

$$x^{1/2}\Theta_{f,yy} + \frac{1}{2}F\Theta_{f,y} = Hx^{1/2}(\Theta_f-\Theta_p) + x(F_y\Theta_{f,x} - \Theta_{f,y}F_x), \tag{26c}$$

$$x^{1/2}\Theta_{p,yy} + \frac{1}{2}G\Theta_{p,y} = \gamma Hx^{1/2}(\Theta_p-\Theta_f) + x(G_y\Theta_{p,x} - \Theta_{p,y}G_x). \tag{26d}$$

For a solution valid near the leading edge we will solve Eqs. (24a–f) and (26a–d) using the method of matched asymptotic expansions with matching between the two regimes, which are $\eta = O(1)$ and $y = O(1)$ as $x \to 0$, and subject to the boundary conditions

$$f = 0, \quad g = 0, \quad \theta_f = 1, \quad \theta_p = 1 \quad \text{at } \eta = 0, \tag{27}$$

$$\Theta_f, \quad \Theta_p \to 0 \quad \text{as } y \to \infty. \tag{28}$$

The following power series expansions in terms of x are now assumed:

$$f(x,\eta) = f_0(\eta) + x^{1/2}f_1(\eta) + xf_2(\eta) + \cdots, \tag{29}$$

$$F(x,y) = F_0(y) + x^{1/2}F_1(y) + xF_2(y) + \cdots, \tag{30}$$

with corresponding expressions for g, G, θ_f, θ_g, Θ_f, Θ_p. When $\eta = O(1)$ as $x \to 0$ we obtain the main boundary layer, termed the inner layer. The relatively thick region where $y = O(1)$ is termed the outer layer.

At O(1) in the inner layer we obtain the equations

$$(1+\sigma_f)f_0' - \beta\sigma_f g_0' = \tau\theta_{f0} + (1-\tau)\theta_{p0}, \tag{31a}$$

$$-\sigma_f f_0' + \beta\left(\frac{1}{K_r}+\sigma_f\right)g_0' = \tau\theta_{f0} + (1-\tau)\theta_{p0}, \tag{31b}$$

$$\theta_{f0}'' + \frac{1}{2}f_0\theta_{f0}' = 0, \tag{31c}$$

$$\theta_{p0}'' + \frac{1}{2}g_0\theta_{p0}' = 0, \tag{31d}$$

$$f_0(0) = 0, \quad g_0(0) = 0, \quad \theta_f(0) = 1, \quad \theta_p(0) = 1, \tag{31e}$$

$$\theta_{f0}, \quad \theta_{p0} \to 0 \quad \text{as } \eta \to \infty. \tag{31f}$$

The solution method used to solve Eqs. (31a–f) is a standard one, dating back to Cheng and Minkowycz [7] and earlier work on boundary layers.

For the regular (monodisperse) porous medium (the case $\sigma_f = 0$, $K_r = 0$, $\tau = 1$) the system of equations reduces to

$$f_0' = \theta_0, \quad \theta_{f0}'' + \frac{1}{2}f_0\theta_{f0}' = 0, \quad \theta_{p0} = 1. \tag{32a, b, c}$$

The solution of this system was presented by Cheng and Minkowycz [7]. The features of interest are that

$$f_0 \to 1.61613 \quad \text{as } \eta \to \infty, \tag{33a}$$

$$\theta_0'(0) = -0.44378, \tag{33b}$$

and θ_0 becomes exponentially small as $\eta \to \infty$. The numerical values are those obtained by Rees and Pop [8].

4. Numerical results

It is noteworthy that the parameters H and γ, the ones associated with local thermal non-equilibrium, do not enter the system of equations (31). Nevertheless there remain four parameters. In this pioneering study we present numerical results, obtained by numerical solution of the system (31) with the geometrical parameters given fixed values, chosen to be $\phi = 0.4$ and $\varepsilon = 0.4$, so that $\tau = 0.625$. Representative results are given in Table 1.

Some information about the magnitude of the inter-phase heat transfer coefficient h in practical cases is available (see, for example, Section 2.2.2 in Nield and Bejan [13]), but no similar information on the magnitude of the inter-phase momentum coefficient ζ has been published.

The following features may be noted. The case $\beta = K_r = 1$ with any value of σ_f gives values approximating those for a regular porous medium. We refer to these as the standard values. In a practical situation, K_r and σ_f are expected to be small compared with unity. In this case, $g_0(\infty)/f_0(\infty) = K_r/\beta$, while $\theta_{p0}'(0)/\theta_{f0}'(0)$ is of order 0.2. Compared with standard values, the values of $\theta_{f0}'(0)$ are

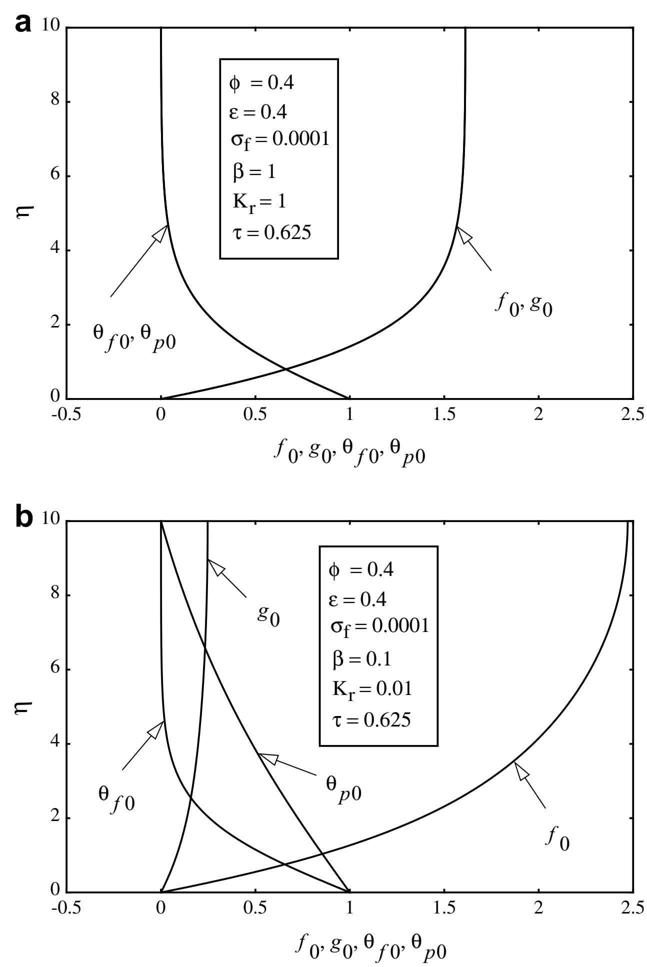

Fig. 2. Plots of temperature and streamfunction profiles for (a) a case approximating a regular porous medium, and (b) a case typical of a bidisperse porous medium.

Table 2
Numerical results obtained from the solution of the system (31) for $\phi = 0.004$, $\varepsilon = 0.4$, and so for $\tau = 0.00994$

Case	σ_f	β	K_r	$f_0(\infty)$	$g_0(\infty)$	$-\theta'_{f0}(0)$	$-\theta'_{p0}(0)$	$-\phi\theta'_{f0}(0) - (1-\phi)\theta'_{p0}(0)$
1	0.0001	0.1	0.0001	4.94742	0.00495	0.54005	0.10062	0.10238
2	0.0001	0.1	0.01	3.86017	0.38609	0.52585	0.15741	0.15889
3	0.0001	0.1	1	0.53389	5.33889	0.25357	1.40695	1.40234
4	0.0001	1	0.0001	4.96029	0.00046	0.54019	0.10006	0.10182
5	0.0001	1	0.01	4.82223	0.04823	0.53871	0.10617	0.10790
6	0.0001	1	1	1.61154	1.61154	0.44390	0.44390	0.44390
7	0.0001	10	0.0001	4.96158	0.00005	0.54020	0.10000	0.10177
8	0.0001	10	0.01	4.94743	0.00495	0.54005	0.10062	0.10238
9	0.0001	10	1	3.86063	0.38606	0.52588	0.15741	0.15888
10	0.01	0.1	0.0001	4.89886	0.00500	0.53728	0.10063	0.10237
11	0.01	0.1	0.01	3.81479	0.38903	0.52296	0.15792	0.15938
12	0.01	0.1	1	0.53389	5.33889	0.25357	1.40695	1.40234
13	0.01	1	0.0001	4.91172	0.00050	0.53741	0.10006	0.10181
14	0.01	1	0.01	4.77420	0.04869	0.53594	0.10623	0.10795
15	0.01	1	1	1.61154	1.61154	0.44390	0.44390	0.44390
16	0.01	10	0.0001	4.91301	0.00005	0.53743	0.10000	0.10176
17	0.01	10	0.01	4.89935	0.00500	0.53730	0.10063	0.10237
18	0.01	10	1	3.86063	0.38606	0.52588	0.15741	0.15888
19	1	0.1	0.0001	2.47349	0.00742	0.37410	0.10093	0.10202
20	1	0.1	0.01	1.77690	0.52262	0.35540	0.18220	0.18290
21	1	0.1	1	0.53389	5.33888	0.25357	1.40695	1.40234
22	1	1	0.0001	2.48313	0.00074	0.37431	0.10009	0.10119
23	1	1	0.01	2.41650	0.07107	0.37494	0.10920	0.11026
24	1	1	1	1.61154	1.61154	0.44390	0.44390	0.44390
25	1	10	0.0001	2.48410	0.00007	0.37433	0.10001	0.10111
26	1	10	0.01	2.51001	0.00738	0.37705	0.10093	0.10203
27	1	10	1	3.86063	0.38606	0.52588	0.15741	0.15888

some 10% higher and those of $f_0(\infty)$ are higher by something of the order of 50%, and in each case the amount of increase depends weakly on the values of β and K_r. The table shows that, for practical values of K_r, a change in σ_f from 0.0001 to 0.01 produces little change in the solution.

In the last column of Table 1 we have presented the representative-elementary-volume average of $\theta'_{f0}(0)$ and $\theta'_{p0}(0)$, namely $\phi\theta'_{f0}(0) + (1-\phi)\theta'_{p0}(0)$. This is a measure of the heat flux at the wall.

In Fig. 2a, we have presented the temperature and streamfunction profiles for Case 6 (see Table 1), which are close to the standard functions (corresponding to a regular porous medium). The profiles for the f-phase and the p-phase are identical. In Fig. 2b, which is computed for Case 2, are the profiles for a typical BDPM. The streamfunction profiles for the two phases are similar and are relatively scaled by the ratio K_r/β, which in this case has the value 0.1. In contrast, the temperature profiles for the two phases are quite different. The profile for the f-phase exhibits a fairly narrow boundary layer behavior, whereas the profile for the p-phase the decay as η increases is much less rapid, and in fact the profile is approximately linear out to a value $\eta = 10$. The fact that there is any exponential decay at all here is a consequence of the bidispersivity of the porous medium. (As Rees and Pop [8] demonstrated, for a regular porous medium the solid-phase temperature decays linearly, not exponentially, at this order of approximation.)

A reviewer commented that for double porosity/permeability aquifers the fractures porosity is often several orders of magnitude smaller than the primary porosity ($\phi \ll \varepsilon$). Results for an illustrative case are presented in Table 2. A comparison with Table 1 reveals some quantitative differences but qualitative similarity in general. One significant trend appears. Comparison of the last three columns of each table shows that the individual f-phase and p-phase heat transfers differ little between the two tables, but the REV-averaged heat transfer changes because it is necessarily dominated by the p-phase value when ϕ is small.

5. Conclusions

We have initiated a study of external natural convection in a bidisperse porous medium, involving convection past a semi-infinite vertical wall. For simplicity, the Darcy model rather than the Brinkman model has been employed. The boundary layer analysis has been presented in a general form. A large number of parameters are involved. In this pioneering study we have confined our attention to the leading edge region. As Rees and Pop [10] have emphasized, what happens near the leading edge sets the scene for what happens further down stream. Within the leading edge region, we have concentrated on what Rees and Pop [8] call the main boundary layer, the inner layer in the asymptotic analysis. For this layer the solution is of similarity type and involves four BDPM parameters, namely the geometrical parameter τ, the inter-phase momentum transfer parameter σ_f, the porosity-modified thermal diffusivity ratio β, and the permeability ratio K_r. A regular porous medium corresponds to the limiting case where $1-\tau$, σ_f and K_r are all small compared with unity. The similarity equations have been solved numerically for representative values of the four parameters.

The stage has been set for future work following the route blazed by Rees and Pop [8]. This would involve the completion of a matched asymptotic analysis for the leading edge region, a numerical solution for an intermediate region, and a further asymptotic analysis for the region far from the leading edge.

A referee has drawn our attention to a number of aspects that could be topics for further study. The analysis can be extended to the case of a porous medium that is characterized by two different permeabilities in the same Representative Elementary Volume. One example would be an aquifer composed of a matrix with a primary porosity (our p-phase) and a dense network of fractures (our f-phase). Another example would be a network of fractures of large aperture (f-phase) and a second system of fractures of smaller aperture (p-phase). Some relevant analysis has been published in [14–17].

Another possible extension would be to transient flow in double permeability media when there is hydraulic non-equilibrium, so that each phase has a distinct value of the pressure and the consequent pressure difference causes an inter-phase mass exchange. The reader is again referred to [14–17].

The referee also noted that we have assumed constant values for the thermal conductivities. A further extension could be to the case where the relevant Péclet number takes large values and thermal dispersion results in the thermal conductivity being velocity dependent [18,19].

References

[1] Z.Q. Chen, P. Cheng, C.T. Hsu, A theoretical and experimental study on stagnant thermal conductivity of bi-dispersed porous media, Int. Commun. Heat Mass Transfer 27 (2000) 601–610.

[2] Z.Q. Chen, P. Cheng, T.S. Zhao, An experimental study of two phase flow and boiling heat transfer in bi-disperse porous channels, Int. Commun. Heat Mass Transfer 27 (2000) 293–302.

[3] D.A. Nield, A.V. Kuznetsov, Forced convection in a bi-disperse porous medium channel: a conjugate problem, Int. J. Heat Mass Transfer 47 (2004) 5375–5380.

[4] D.A. Nield, A.V. Kuznetsov, A two-velocity two-temperature model for a bi-dispersed porous medium: forced convection in a channel, Transp. Porous Media 59 (2005) 325–339.

[5] D.A. Nield, A.V. Kuznetsov, The onset of convection in a bidisperse porous medium, Int. J. Heat Mass Transfer 49 (2006) 3068–3074.

[6] D.A. Nield, A.V. Kuznetsov, Heat transfer in bidisperse porous media, in: D.B. Ingham, I. Pop (Eds.), Transport Phenomena in Porous Media III, Elsevier, Oxford, 2005, pp. 34–59.

[7] P. Cheng, W.J. Minkowycz, Free convection about a vertical plate imbedded in a porous medium with application to heat transfer from a dyke, J. Geophys. Res. 82 (1977) 2040–2044.

[8] D.A.S. Rees, I. Pop, Vertical free convective boundary-layer flow in a porous medium using a thermal nonequilibrium model, J. Porous Media 3 (2000) 31–44.

[9] A.A. Mohamad, Natural convection from a vertical plate in a saturated porous medium: non-equilibrium theory, J. Porous Media 4 (2001) 181–186.

[10] D.A.S. Rees, I. Pop, Comments on "Natural convection from a vertical plate in a saturated porous medium: non-equilibrium theory" by A.A. Mohamad, J. Porous Media 5 (2002) 225–227.

[11] O.M. Haddad, M.A. Al-Nimr, A.N. Al-Khateeb, Validation of the thermal equilibrium assumption in natural convection from a vertical plate embedded in a porous medium: non-Darcian model, Int. J. Heat Mass Transfer 74 (2004) 2037–2042.

[12] O.M. Haddad, M.A. Al-Nimr, A.N. Al-Khateeb, Validity of the local thermal equilibrium assumption in natural convection from a vertical plate embedded in a porous medium, J. Porous Media 8 (2005) 85–95.

[13] D.A. Nield, A. Bejan, Convection in Porous Media, third ed., Springer, New York, 2006.

[14] H.H. Gerke, M.T. van Genuchten, Evaluation of a first order transfer term for variably saturated dual porosity flow models, Water Resour. Res. 29 (1993) 1225–1238.

[15] M. Bai, D. Elsworth, J.C. Roegiers, Multiporosity/multipermeability approach to the simulation of naturally fractures reservoirs, Water Resour. Res. 29 (1993) 1621–1633.

[16] H. Onder, One-dimensional transient flow in a finite fractures aquifer system, Hydrol. Sci. 43 (1998) 243–265.

[17] K.N. Moutsopoulos, A.A. Konstantinidus, I. Meladiotis, C.D. Tzimopoulos, E.C. Aifantis, On the numerical solution and qualitative behaviour of double porosity aquifers, Transp. Porous Media 42 (2001) 265–292.

[18] D.L. Koch, J.F. Brady, Dispersion in fixed beds, J. Fluid. Mech. 154 (1985) 399–427.

[19] K.N. Moutsopoulos, D.L. Koch, Hydrodynamic and boundary layer dispersion in bidisperse porous media, J. Fluid. Mech. 385 (1999) 359–379.